Available online at www.sciencedirect.com
ScienceDirect
Icarus 192 (2007) 223–237
ICARUS
www.elsevier.com/locate/icarus

New findings on asteroid spin-vector distributions

A. Kryszczyńska [a,*], A. La Spina [b], P. Paolicchi [c], A.W. Harris [d], S. Breiter [a], P. Pravec [e]

[a] *Astronomical Observatory, Adam Mickiewicz University, Słoneczna 36, 60-286 Poznań, Poland*
[b] *Dipartimento di Matematica, Università di Pisa, via Buonarroti 2, I-56127 Pisa, Italy*
[c] *Dipartimento di Fisica, Università di Pisa, Largo Pontecorvo 3, I-56127 Pisa, Italy*
[d] *Space Science Institute, 4603 Orange Knoll Ave., La Canada, CA 91011-3364, USA*
[e] *Astronomical Institute AS CR, Fricova 1, CZ-25165 Ondrejov, Czech Republic*

Received 15 February 2007; revised 15 June 2007

Available online 25 July 2007

Abstract

The number of known spin vectors of main belt and near-Earth asteroids is regularly growing, including new objects, and updating the estimates concerning known cases, with the aid of new observations and of improved observational techniques. A reliable statistical analysis of the spin vectors is now possible. In general the poles (both for MB bodies and for NEAs) are not isotropically distributed, as some general theoretical considerations may predict. Main belt asteroids show a lack of poles close to the ecliptic plane. There is a marginally significant excess of prograde spinners in the 100–150 km size range, but interestingly there is not a statistically significant excess in the larger size range. Among NEAs, there is an excess of retrograde rotations. The distributions of longitudes of poles of both groups do not show statistically significant deviations from random. We discuss the possible physical implications of the various resulting pole anisotropies in terms of dynamical—mainly non-gravitational—effects, and point out the importance of new observational campaigns, mainly devoted to compute the poles of small bodies and of the members of asteroid dynamical families.

Keywords: Asteroids, rotation

1. Introduction

Photometric lightcurves of asteroids provide information about rotational periods, orientations of spin axes and shapes, as well as of the physical properties of their surfaces. Photometric methods have been supported and tested by a variety of other observational techniques (for example, with respect to the rotational properties, radar observations and spacecrafts flybys).

Prior to about 2000, it was presumed that the spin properties of asteroids depend mainly on their collisional evolution (Davis et al., 1989); this would predict a nearly isotropic distribution of poles. A small excess of prograde spins might be expected, especially for large main belt asteroids (MBAs), due to a residual directed component of spins from the time of formation. But, in reality, the magnitude of the "directed component" might be only of the order of the orbital frequency, and thus be completely overwhelmed by the isotropic component of spin due to random collisions (see, for example, Bertotti et al., 2003). Asteroid collisional evolution studies are aimed at understanding how collisions have shaped the observed features of the asteroid population, in order to support models of the formation and evolution of the Solar System (Davis et al., 2002). Changes in the spin rate and the creation of tumbling rotation states and of binary asteroids are among the consequences of collisions (Paolicchi et al., 2002).

Early statistical analyses of the asteroid spin-vector distributions were performed by Magnusson (1986, 1990) and Drummond et al. (1988, 1991). The studies were based on no more than 30 asteroids and showed a bi-modality of the observed pole distribution and an apparent lack of poles close to the ecliptic plane. Analyses performed by Pravec et al. (2002), based on 83 objects, have confirmed the earlier findings. Detailed analyses for 73 main belt asteroids have also been made by Skoglov and Erikson (2002) (see Section 3).

* Corresponding author. Fax: +48 61 8292772.
E-mail address: agn@amu.edu.pl (A. Kryszczyńska).

0019-1035/$ – see front matter
doi:10.1016/j.icarus.2007.06.008

2. Data

A database of asteroid spin-vector determinations was originally created by Per Magnusson, at that time working at the Uppsala Observatory (Sweden) and reported in the *Asteroids II* book (Magnusson, 1989). The latest update of his data set was made in December 1995 and contained the poles (expressed in terms of the geocentric ecliptic coordinates of the pole) and in many cases also sidereal periods of rotation and shapes (but only when part of a spin-vector determination) for about 100 asteroids. It is still available at the archives of the Small Bodies Node of the NASA Planetary Data System: http://pdssbn.astro.umd.edu/.

Recently, the maintenance and updating of this data set has been adopted by the Poznań Observatory (Poland). All new asteroid pole determinations found in the literature have been included. At the present time the list (which is regularly updated) contains pole coordinates and supplementary information for about 170 asteroids and is available at: http://www.astro.amu.edu.pl/Science/Asteroids/.

For most asteroids several independent solutions have been published. This can be confusing for non-specialists and readers not interested in the spin-vector determination process. Because of this and also to ease statistical studies, "synthesis values" (estimated at the best of our present knowledge) have been added for some asteroids. The synthesis values have been obtained by taking averages of the most recent independent results, with weights based on the reliability of the method used and the amount of the input data. This process is somewhat subjective but has been based on regular discussions with several experts in pole determination. Table 1 presents a sample page of the main table of the list. In the first column the method of the pole vector determination is indicated (A—amplitude, M—magnitude, E—epoch, L—lightcurve inversion, R—radar methods, etc.). In the following columns we have places for four different spin vector solutions per line: two for prograde ($\beta_0 > 0$) and two for retrograde rotation ($\beta_0 < 0$). These reflect the symmetry properties of most of the spin-vector determination methods. In the next column we have the sidereal period of rotation given in days and the shape approximated by a triaxial ellipsoid. For a few asteroids there is evidence of a surface albedo variegation (for example, spots on their surfaces); this fact can be indicated in the column number 13. The last column gives the reference codes fully described in the reference list.

In Table 1 we have spin vector solutions for seven asteroids. For three of them (88 Thisbe, 107 Camilla and 125 Liberatrix) the syntheses are the average values of the independent results. In the case of 115 Thyra the maximum weight was given to the latest pole determination, based on input data improved by the lightcurves obtained during 4 new oppositions (Michałowski et al., 2004). For three objects (108 Hecuba, 110 Lydia, 121 Hermione) the amount of the input data was insufficient to obtain a reliable sense of rotation and a sidereal period: future observations are required.

In the course of compiling published pole solutions, we have developed a "certainty scale" as follows: 0—either wrong or very uncertain determination, 1—possible but not certain pole determination, 2—good determination, based on a large dataset, two equally probable solutions are available (different in both latitude and longitude), 3—very good determination, based on a large dataset, an ambiguity of about 180° in pole longitude might appear, 4—excellent determination, pole position confirmed by the methods based on independent datasets (for example, lightcurves and radar data, lightcurves and spacecraft fly-by).

Our assignment of a code is based on the quality of the data, the pole solution method used, and on the consistency of results from multiple analyses. These assignments are necessarily somewhat subjective, but we feel necessary in order to limit our analysis to only reasonably reliable determinations. Most of the poles we used for our analyses have reliability codes 3, and none less than 2. The data are also given in Appendix A.

3. Previous analyses and physical problems

The first analyses of the asteroid spin-vector distribution (done by, e.g., Zappala and Knezevic, 1984; Barucci et al., 1986), based on small number of objects, suggested a depopulation of poles close to the ecliptic plane. The analysis of the earlier data (Magnusson, 1986, 1989, 1990) showed evidence of a significant deviation from an isotropic distribution in ecliptic latitude of the spin vector orientations, being preferentially clustered toward the ecliptic poles. At the time it seemed possible that this might be due to a selection effect related to the method of analysis. A more recent analysis has been presented by Pravec et al. (2002), based on 83 asteroids, with many poles re-determined with more extensive lightcurve data sets and good pole determination algorithms. However, the qualitative scenario remains the same. The first suggestion of a deviation from isotropy with respect to ecliptic longitudes is due to Binzel (1987, unpublished presentation at a workshop on catastrophic disruption, in Belgrade), relating to pole orientations of members of the Koronis family. More recently, Samarasinha and Karr (1998) have suggested some degree of anisotropy in the general main-belt population. The clustering of poles suspected by Binzel has been confirmed by Slivan (2002), and explained by Vokrouhlicky et al. (2003). A recent analysis by La Spina et al. (2004a) has found only small deviations from isotropy for the longitude distribution of MBAs, while showing a bi-modal behavior for near-Earth asteroids (NEAs); however, the poor statistics do not allow definite conclusions.

A detailed analysis has been presented by Skoglov and Erikson (2002), based on a set of 73 asteroids. They discuss the depopulation of spin vectors close to the ecliptic plane, and introduce a possible explanation based on a correlation with the orbital inclination.

They divide their input data into two groups with respect to the orbital inclinations of the objects, those with inclination $I < 10°$ and those with $I > 10°$. The asteroids with high orbital inclinations were found to exhibit a depopulation of vectors close to the ecliptic plane, whereas asteroids with orbits closer to the ecliptic plane (small inclinations) were found to have a more regular spin-vector distribution.

Table 1
The fragment of the main table of the asteroid spin vector determinations data set

Basic data	Spin vector solutions (ecliptic coordinates of equinox 1950)								Sidereal period (days)	Ellipsoidal albedo model variegation		Reference code
	λ_0	β_0	γ_0	β_0	λ_0	β_0	λ_0	β_0		a/b	b/c	
88 Thisbe												
AM	32°	+69°	205°	+54°	25°	−54°	212°	−69°	–	1.13	1.0[1]	Za + 86b
EAM			129°	+78°	E	E	E	E	0.2517222	1.12	1.30	Dr + 88b
EA	40°	+70°	200°	+70°	E	E	E	E	0.2517223	1.13		Mag90a
EAM			110°	+58°	E	E	E	E	0.2517222	1.15	1.16	Dru + 91
EA			243°	+74°	E	E	E	E	0.2517224	1.11	1.22	DeA95
L			207°	+48°					0.2517208	1.1	1.2[31]	Tor + 03
Synthesis			190°	+64°	E	E	E	E	0.25172	1.1	1.2	Synthesis
107 Camilla												
EAM	71°	+61°	233°	+74°	E	E	E	E	0.2018306	1.45	1.72	Dr + 88b
EAM	74°	+55°	239°	+76°	E	E	E	E	0.2018305	1.46	1.6	Mag90a
EAM			229°	+73°	E	E	E	E	0.2018305	1.47	1.49	Dru + 91
EA			230°	+69°	E	E	E	E	0.2018307	1.46	1.58	DeA95
L	72°	+51°							0.2018304	1.4	1.2	Tor + 03
Synthesis	72°	+56°	232°	+72°	E	E	E	E	0.2018306	1.46	1.6	Synthesis
108 Hecuba												
AM	79°	+13°					259°	−13°	–	1.180	1.101	Bla + 98
AM	79°	+6°					259°	−6°	–	1.180	1.101	Bla + 98
110 Lydia												
EAM	24°	+75°	210°	+78°					–	1.17		Mic96a
115 Thyra												
EA	175°	+60°	330°	+60°	E	E	E	E	0.301565	1.14	1.30	Dot + 95
AM	197°	+30°	358°	+35°	17°	−30°	178°	−35°	–	1.224	1.088	Bla + 98
EAM							182°	−43°	0.3017940	1.21	1.03	Mic + 03
EAM	7°	+34°							0.3017257	1.23	1.03	Mic + 04
L	23°	+33°							0.3016652	1.1	1.1[31]	Mic + 04
Synthesis	15°	+34°							0.30169	1.2	1	Synthesis
121 Hermione												
EA	163°	+12°	342°	+30°	162°	−30°	343°	−12°	–	1.10	1.00	DeA95
AM	40°	+32°					220°	−32°	–	1.294	1.288	Bla + 96
AM			240°	+42°	60°	−42°			–	1.294	1.393	Bla + 98
125 Liberatrix												
EAM	80°	+74°			E	E	E	E	0.1653422	1.28	2.68	Dr + 88b
E		+70°		+70°	E	E	E	E	0.1653425			Mag90a
EAM			228°	+71°	E	E	E	E	0.1653420	1.35	1.23	Dru + 91
EA	15°	+47°	181°	+53°	E	E	E	E	0.1653418	1.55	1.10	DeA95
Synthesis	48°	+64°	205°	+65°	E	E	E	E	0.1653422			Synthesis

This fact was explained as due to differences in the dynamic evolution of the spin vectors between objects with high and low orbital inclinations. However, as we will discuss later, a similar analysis involving the objects included in the present dataset does not confirm the significance of the inclination effect on the distribution of pole latitudes.

As mentioned in Section 1, from the theoretical point of view, it is reasonable to envisage a nearly isotropic distribution of poles, with—maybe—a very small excess of prograde rotators due to a small directed component of spin, presumed to be prograde-upright.

According to recent analyses, the processes connected with reflection or reemission of solar radiation from an asteroid surface, and in particular the Yarkovsky effect, can affect the asteroids' dynamical evolution, causing orbital changes. The Yarkovsky effect can indirectly affect the spin vector properties as well. For instance, it has been argued that the excess of retrograde rotators among near-Earth asteroids can be explained in terms of a selection of the asteroids transferred into the NEA region, due to the Yarkovsky effect (La Spina et al., 2004b). The amount of the retrograde excess that they have found confirms the quantitative estimates on the relative importance of the different injection channels, presented in earlier theoretical studies (Bottke et al., 2002; Morbidelli and Vokrouhlicky, 2003). The knowledge of the spin vector might also be useful to identify the region, in the main belt, from which a given NEA has originated (Marchi et al., 2005).

A process related to the Yarkovsky effect, the so-called YORP (Yarkovsky–O'Keefe–Radzievskii–Paddack) effect, has been shown to be capable of directly affecting the spin rates and

spin axis orientations of moderately sized asteroids (Rubincam, 2000). A process of this kind might dominate the spin evolution of bodies smaller than about 40 km in diameter and has been claimed to explain the spin vector properties of the Koronis family asteroids (Slivan, 2002; Vokrouhlicky et al., 2003).

4. Pole distribution analysis

4.1. Latitude distribution

The distribution of the latitudes is strongly anisotropic. In Fig. 1 we show the updated distribution of the ecliptic latitudes for 92 MBAs, following the same conventions adopted in Pravec et al. (2002). We treat as MBAs all objects with semimajor axes from 2.20 to 3.91 AU that are not indicated in the last column of Table 2 as Amor, Apollo or Aten. The distribution shows a moderate excess of prograde spins and a strong depopulation of poles close to the ecliptic plane, thus confirming previous findings. The excess of prograde spins in the sample is, according to simple statistical considerations, not far from a "2-σ" significance ($\sigma^2 \simeq Np(1-p)$, where N is the total number of objects in the sample and $p = 0.5$ is the probability—a priori—of being prograde or retrograde). The deficit of bodies close to the ecliptic (bin 4) is definitely significant (1.5 objects instead of the expected 13 or 14). In the figure we also plot the distribution of the "orbital latitudes," computed with reference to the real orbital plane of each asteroid. In case of an ambiguous pole solution (most often the ambiguity concerns only the pole longitude) each value is counted with a weight of 0.5. We also plot the ecliptic latitude distribution for those asteroids for which an unambiguous assignment of the latitude zone is possible. The qualitative properties of the three distributions are very similar to each other.

Magnusson (1986) suggested that a part of the effect of depopulation of poles close to the ecliptic plane could be due to a systematic error introduced by the amplitude and magnitude methods of pole determination and also suspected that there exists an observational bias introduced by the epoch method's inability to use near-zero-amplitude lightcurves obtained for objects with the spin axis near the ecliptic plane.

However, the techniques of analysis have continued to improve and the available data set to increase, thus one would expect that the significance of a selection effect such as the one mentioned above would decrease with time. Instead the depopulation appears to remain, and in fact gain in statistical significance, suggesting that it is real.

In a recent paper (La Spina et al., 2002) the distribution has been compared with a bi-variate one, allowing a best-fit mean value different from zero and a different variance in one direction. For the discussion of this point and of the other possible consequences, see the above quoted paper.

We have also tested the often repeated claim that there is a prograde excess among the very largest asteroids, as a remnant of the formation processes. In Fig. 2 we have plotted the cumulative excess of prograde vs retrograde asteroids larger than a given size, as a function of the size (thus the number

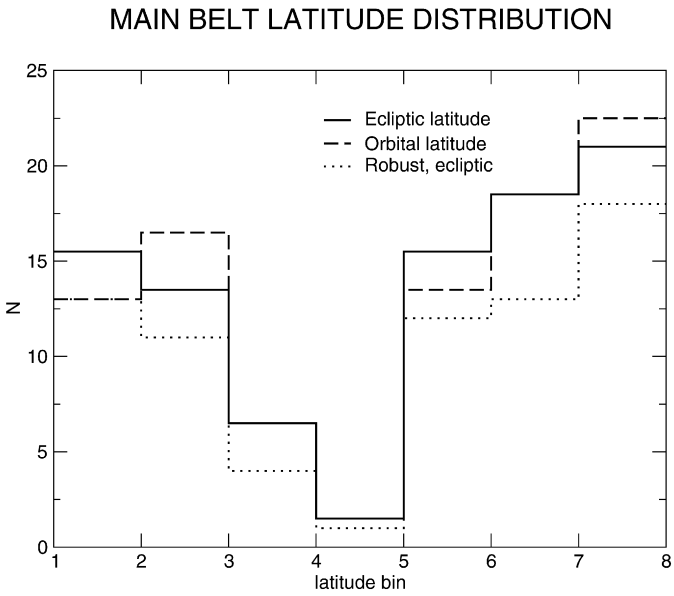

Fig. 1. The histogram shows (solid lines) the distribution of the ecliptic latitude for the poles of 92 main belt asteroids (MBAs). Whenever the computations give an ambiguous (two-fold) pole designation either value is counted with a weight of 0.5. The zones referred to in the abscissa are defined with the same conventions as in Pravec et al. (2002), representing approximately equal surfaces on the λ, β sphere; region 1 means retrograde, from $-90°$ to $-45°$, 2 means -45 to -25, 3 means -25 to -8, 4 means -8 to 8 (prograde) and so on. The histogram shows also the latitude distribution computed with respect to the asteroid orbital plane (long dashed lines) and the ecliptic latitude distribution for the cases in which, also in presence of ambiguous determinations, the latitude zone is uniquely identified (dotted lines).

of included bodies *increases* with decreasing size). We compare the curve to an estimate of the standard statistical error (essentially the square root of the number of bodies). It can be seen that the excess is within—or close to—the standard error for the largest bodies, while undergoing a sudden—and formally significant—increase around 100–150 km. We have analyzed in some detail this group of bodies, looking for an explanation of this feature. At the moment we have not found any physical explanation nor any significant correlation with other properties (even if we recall that in this region the spin rate distribution is rather perturbed—the minimum of the mean spin rate as function of the size is close to 100 km). Thus it is not clear whether it is due to a chance statistical fluctuation, of about "2.5-σ" significance at its peak, or due to a real—but not yet understood—physical process. Perhaps the most important result coming out of this analysis is the lack of any significant preference for prograde spin among the largest asteroids, down to a diameter of about 200 km or even smaller. Thus, if the spins of the largest asteroids keep, at least partially, memory of their primordial properties (and probably it is so), one must conclude that those spins were essentially isotropic, in agreement with the theory (Bertotti et al., 2003).

In Fig. 3 we plot the latitude distributions for 21 NEAs (the same cases presented for MBAs). The NEAs exhibit a strong excess of retrograde, instead of prograde, bodies. This discrepancy, which is statistically meaningful, has already been discussed by La Spina et al. (2004b).

Table 2
Summary of the data used in the analysis

Asteroid	λ_e	β_e	q	z_e	D	λ_o	β_o	z_o	ν	I	e	A	Ω	$\dot{\Omega}$	a/b	b/c	$\langle\dot{\psi}\rangle$	β_{min}	β_{max}	M	Taxonomy, family
1 Ceres	332	70	3	7	848	234	80	7	2.6446	10.6	0.08	2.77	80	−59.185	1.08	1.06	7.4	57.	81.	0	C, G Ceres
2 Pallas	44	−9	3	3	498	229	18	5	3.0717	34.9	0.23	2.77	173	−45.554	1.10	1.05	−0.49	−42.	26.	0	B
3 Juno	106	34	3	6	234	301	45	6	3.3289	13.0	0.26	2.67	170	−61.820	1.20	1.30	11.	15.	47.	0	Sk
4 Vesta	326	53	4	7	468	213	57	7	4.4926	7.1	0.09	2.36	104	−39.590	1.10	1.20	13.	40.	61.	0	V
5 Astraea	123	51	3	7	119	348	52	7	1.4285	5.4	0.19	2.57	142	−59.347	1.30	1.15	36.	35.	64.	0	S
	319	49		7		171	48	7									37.	36.	66.	0	
6 Hebe	355	41	3	6	185	203	48	7	3.2992	14.8	0.20	2.43	139	−41.973	1.17	1.10	9.7	19.	58.	0	S
7 Iris	15	28	2	6	200	114	23	5	3.3619	5.5	0.23	2.39	260	−46.353	1.20	1.20	13.	22.	38.	0	S
	196	10		5		297	15	5									4.5	3.5	16.	0	
8 Flora	140	22	3	5	136	31	19	5	1.8751	5.9	0.16	2.20	111	−35.280	1.05	1.20	25.	14.	49.	0	S Flora
9 Metis	182	26	2	6	170	112	21	5	4.7252	5.6	0.12	2.39	69	−41.994	1.30	1.30	11.	20.	36.	0	S
	360	11		5		291	16	5									4.2	4.	16.	0	
10 Hygiea	111	−36	3	2	407	190	−35	2	0.8688	3.8	0.12	3.14	284	−94.345	1.29	1.10	−22.	−39.	−32.	0	C Hygiea
	298	−37		2		11	−38	2									−23.	−40.	−34.	0	
12 Victoria	150	50	3	7	113	275	58	7	2.7712	8.4	0.22	2.33	236	−40.856	1.30	1.20	23.	19.	58.	0	L, S Victoria
15 Eunomia	106	−74	3	1	255	211	−71	1	3.9456	11.7	0.19	2.65	293	−51.995	1.42	1.10	−16.	−83.	−65.	0	S
	353	−60		1		45	−69	1									−15.	−71.	−53.	0	
16 Psyche	35	−15	3	3	253	245	−12	3	5.1798	3.1	0.14	2.92	150	−73.064	1.25	1.25	−2.7	−18.	−12.	0	X, M
	216	−10		3		66	−13	3									−1.9	−13.	−7.2	0	
17 Thetis	58	12	2	5	90	293	17	5	1.9566	5.6	0.13	2.47	126	−46.396	1.30	1.00	4.6	5.1	18.	0	Sl
	240	25		5		113	20	5									10.	19.	34.	0	
18 Melpomene	190	−20	2	3	141	36	−26	2	2.0741	10.1	0.22	2.30	151	−39.596	1.20	1.20	−17.	−29.	−15.	0	S
	355	−37		2		210	−32	2									−27.	−41.	−29.	0	
19 Fortuna	80	52	3	7	226	228	53	7	3.2244	1.6	0.16	2.44	211	−45.208	1.20	1.00	8.3	50.	53.	0	Ch, G
	260	52		7		50	51	7									8.4	51.	54.	0	
20 Massalia	23	59	3	7	146	175	59	7	2.9638	0.7	0.14	2.41	207	−45.050	1.15	1.10	16.	58.	60.	0	S Massalia
	203	60		7		357	60	7									16.	59.	61.	0	
21 Lutetia	42	10	3	5	96	321	12	5	2.9390	3.0	0.16	2.44	81	−44.656	1.25	1.20	5.1	6.5	13.	0	Xk, M
	225	10		5		144	8	4									5.2	6.6	13.	0	
22 Kalliope	21	−22	2	3	181	312	−12	3	5.7856	13.7	0.10	2.91	66	−62.930	1.30	1.20	−3.1	−34.	−8.4	0	X, M
	193	0		4		128	−11	3									0.012	−14.	14.	0	
23 Thalia	7	−55	3	1	108	294	−46	1	1.9489	10.1	0.23	2.63	67	−64.361	1.20	1.30	−32.	−59.	−45.	0	S
28 Bellona	83	18	2	5	121	300	26	6	1.5291	9.4	0.15	2.78	145	−66.854	1.20	1.20	9.9	5.4	28.	0	S
	275	40		6		126	33	6									24.	30.	60.	0	
29 Amphitrite	136	−28	4	2	212	142	−32	2	4.4526	6.1	0.07	2.55	357	−47.131	1.10	1.10	−4.3	−34.	−23.	0	S
31 Euphrosyne	273	−60	3	1	256	253	−36	3	4.3387	26.3	0.23	3.15	31	−60.400	1.09	1.60	−8.8	−79.	−34.	0	Cb, C
32 Pomona	92	45	3	6	81	227	49	7	2.5403	5.5	0.08	2.59	221	−50.366	1.30	1.30	22.	32.	52.	0	S
	262	58		7		47	54	7									29.	50.	76.	0	
37 Fides	85	−26	2	2	108	78	−29	2	3.2727	3.1	0.18	2.64	7	−57.680	1.10	1.05	−3.7	−29.	−23.	0	S
	264	−34		2		257	−31	2									−4.6	−37.	−31.	0	
39 Laetitia	324	31	3	6	150	161	28	6	4.6709	10.4	0.11	2.77	157	−56.403	1.40	1.40	8.8	19.	44.	0	S
40 Harmonia	17	31	2	6	108	284	35	6	2.6937	4.3	0.05	2.27	94	−35.182	1.30	1.00	10.	23.	35.	0	S
	204	33		6		109	29	6									12.	29.	42.	0	
41 Daphne	194	−31	3	2	174	6	−34	2	4.0080	15.8	0.27	2.76	178	−76.619	1.30	1.10	−6.3	−46.	−17.	0	Ch, C
	342	−34		2		175	−37	2									−6.9	−49.	−20.	0	

(*continued on next page*)

Table 2 (*continued*)

Asteroid	λ_e	β_e	q	z_e	D	λ_o	β_o	z_o	ν	I	e	A	Ω	$\dot{\Omega}$	a/b	b/c	$\langle\dot{\psi}\rangle$	β_{min}	β_{max}	M	Taxonomy, family
42 Isis	119	−18	3	3	100	31	−23	3	1.7651	8.5	0.22	2.44	85	−47.284	1.10	1.00	−3.3	−27.	−11.	0	L, S
	291	−20		3		208	−16	3									−3.4	−27.	−12.	0	
43 Ariadne	252	−16	3	3	66	346	−15	3	4.1652	3.5	0.17	2.20	265	−35.363	1.60	1.15	−9.6	−18.	−13.	0	Sk Flora
44 Nysa	100	53	3	7	71	332	55	7	3.7375	3.7	0.15	2.42	132	−46.311	1.40	1.20	21.	45.	58.	0	Xc, E Nysa
	296	52		7		160	51	7									22.	46.	60.	0	
45 Eugenia	119	−34	3	2	215	327	−31	2	4.2112	6.6	0.08	2.72	148	−58.282	1.40	1.50	−12.	−39.	−28.	0	C, FC
	301	−27		2		156	−30	2									−10.	−33.	−22.	0	
47 Aglaja	139	33	3	6	127	134	29	6	1.8197	5.0	0.13	2.88	3	−69.591	1.21	1.20	15.	27.	40.	0	B, C
	313	19		5		311	23	5									8.7	13.	24.	0	
51 Nemausa	160	−64	3	1	148	327	−60	1	3.0836	10.0	0.07	2.37	176	−39.294	1.15	1.00	−7.9	−72.	−55.	0	Ch, CU
	356	−62		1		198	−60	1									−7.7	−70.	−53.	0	
52 Europa	69	28	3	6	303	303	34	6	4.2629	7.5	0.10	3.10	129	−86.972	1.20	1.20	4.1	19.	35.	0	C, CF Hygiea
	258	42		7		125	36	6									6.	34.	51.	0	
54 Alexandra	160	45	3	6	166	194	49	7	3.4157	11.8	0.20	2.71	314	−60.428	1.30	1.00	6.9	31.	58.	0	C
	290	55		7		353	58	7									8.	40.	68.	0	
55 Pandora	30	38	3	6	67	24	35	6	4.9958	7.2	0.14	2.76	11	−59.791	1.25	1.20	7.2	30.	46.	0	X, M
	228	27		6		214	31	6									5.2	19.	34.	0	
60 Echo	95	34	3	6	60	263	38	6	0.9540	3.6	0.18	2.39	192	−46.474	1.50	1.40	97.	38.	45.	2	S
	275	42		6		83	38	6									79.	28.	38.	2	
63 Ausonia	120	−27	3	2	103	145	−30	2	2.5813	5.8	0.13	2.40	338	−41.788	2.10	1.00	−22.	−32.	−24.	0	Sa
	308	−34		2		327	−31	2									−26.	−36.	−29.	0	
64 Angelina	119	29	3	6	140	169	29	6	2.7414	1.3	0.12	2.68	309	−59.756	1.40	1.00	8.2	28.	31.	0	Xe, E
	299	27		6		351	27	6									7.5	25.	28.	0	
65 Cybele	28	−41	3	2	237	234	−38	2	5.9398	3.6	0.10	3.44	156	−159.264	1.07	1.60	−4.6	−44.	−37.	0	Xc, P Cybele
83 Beatrix	4	−42	3	2	81	332	−40	2	2.3732	5.0	0.08	2.43	28	−43.625	1.24	1.10	−18.	−45.	−38.	0	X
	172	−34		2		147	−37	2									−16.	−39.	−31.	0	
85 Io	106	−46	2	1	155	264	−34	2	3.4908	12.0	0.19	2.65	203	−53.166	1.10	1.00	−2.7	−57.	−34.	0	B, FC Eunomia
	293	−15		3		90	−27	2									−1.	−27.	−3.5	0	
87 Sylvia	82	55	3	7	261	23	52	7	4.6299	10.9	0.08	3.49	73	−130.867	1.40	1.10	4.7	44.	66.	0	X, P Cybele
88 Thisbe	190	64	3	7	201	274	69	7	3.9727	5.2	0.16	2.77	277	−63.896	1.10	1.20	11.	57.	69.	0	B, CF
93 Minerva	196	13	3	5	141	190	15	5	4.0120	8.6	0.14	2.75	4	−61.189	1.10	1.05	1.3	4.6	22.	0	C, CU
107 Camilla	72	56	2	7	223	255	66	7	4.9547	10.0	0.08	3.48	173	−140.774	1.45	1.50	7.2	45.	66.	0	X, C Cybele
	232	74		7		70	65	7									8.4	64.	85.	0	
115 Thyra	15	34	3	6	80	68	23	5	3.3147	11.6	0.19	2.38	309	−41.919	1.20	1.00	6.1	22.	49.	0	S
125 Liberatrix	48	64	3	7	44	233	68	7	6.0481	4.7	0.08	2.74	169	−58.175	1.45	1.16	9.9	58.	69.	0	X, M Liberatrix
	205	65		7		43	62	7									10.	60.	71.	0	
129 Antigone	200	65	3	7	125	72	54	7	4.8415	12.2	0.21	2.87	136	−78.213	1.30	1.04	6.6	53.	80.	0	X, M
130 Elektra	190	−84	2	1	182	283	−71	1	4.5936	22.9	0.21	3.12	146	−69.141	1.40	1.20	(78)	−74.	−65.	3	Ch, G
	243	−36		2		101	−59	1									−5.3	−59.	−17.	0	
135 Hertha	100	52	3	7	79	115	50	7	2.8552	2.3	0.21	2.43	344	−46.665	1.15	1.20	22.	50.	58.	0	Xk, M Nysa
	292	50		7		310	52	7									21.	45.	53.	0	
158 Koronis	27	−67	3	1	35	98	−68	1	1.6894	1.0	0.06	2.87	289	−65.696	1.45	1.60	−46.	−68.	−67.	0	S Koronis
	211	−70		1		281	−69	1									−47.	−70.	−69.	0	
167 Urda	39	−74	3	1	40	237	−72	1	1.8375	2.2	0.04	2.85	166	−64.596	1.25	1.00	−13.	−75.	−72.	0	Sk Koronis
	225	−71		1		55	−73	1									−13.	−73.	−70.	0	

Table 2 (*continued*)

Asteroid	λ_e	β_e	q	z_e	D	λ_o	β_o	z_o	ν	I	e	A	Ω	$\dot{\Omega}$	a/b	b/c	$\langle\dot{\psi}\rangle$	β_{min}	β_{max}	M	Taxonomy, family
173 Ino	178	−14	2	3	154	26	−21	2	3.9238	14.2	0.21	2.74	148	−59.574	1.10	1.10	−3.	−35.	−8.5	0	Xk, C
	344	−30		2		203	−25	3									−4.5	−47.	−20.	0	
196 Philomela	277	20	3	5	136	201	23	5	2.8772	7.3	0.02	3.11	73	−80.274	1.30	1.20	5.	12.	28.	0	S
201 Penelope	85	−29	3	2	68	287	−23	3	6.4043	5.8	0.18	2.68	157	−58.331	1.50	1.20	−6.	−33.	−23.	0	M
	260	−21		3		104	−27	2									−4.8	−27.	−16.	0	
208 Lacrimosa	162	−65	3	1	41	161	−66	1	1.7049	1.8	0.01	2.89	5	−67.359	1.35	1.70	−44.	−67.	−65.	0	S Koronis
	346	−68		1		337	−67	1									−45.	−68.	−66.	0	
216 Kleopatra	72	16	2	5	135	212	23	5	4.4566	13.1	0.25	2.79	216	−72.155	2.60	1.30	6.3	0.96	30.	0	X, M
	232	37		6		25	32	6									14.	22.	55.	0	
230 Athamantis	83	36	3	6	109	196	39	6	1.0006	9.4	0.06	2.38	240	−38.017	1.10	1.10	26.	11.	89.	0	Sl
	239	40		6		7	40	6									(14)	16.	76.	4	
243 Ida	262	−68	4	1	28	297	−67	1	5.1795	1.1	0.05	2.86	324	−65.235	1.80	1.20	−14.	−69.	−67.	0	S Koronis
270 Anahita	293	59	3	7	51	42	57	7	1.5936	2.4	0.15	2.20	254	−33.950	1.25	1.28	70.	53.	58.	2	S
277 Elvira	53	−79	3	1	27	187	−79	1	0.8083	1.2	0.09	2.89	232	−67.159	1.40	1.50	−95.	−80.	−79.	1	S Koronis
	245	−78		1		7	−78	1									−94.	−78.	−77.	1	
311 Claudia	24	40	3	6	24	305	43	6	3.1867	3.2	0.01	2.90	81	−67.575	1.80	1.00	12.	36.	44.	0	S Koronis
	209	43		6		126	40	6									12.	39.	47.	0	
321 Florentina	94	−62	3	1	27	51	−64	1	8.3598	2.6	0.04	2.89	40	−66.874	1.45	1.50	−8.3	−64.	−60.	0	S Koronis
	265	−65		1		229	−63	1									−8.5	−67.	−62.	0	
334 Chicago	15	35	3	6	156	242	39	6	2.6093	4.7	0.03	3.91	131	−246.300	1.88	1.40	7.5	30.	40.	0	C Hilda
	184	50		7		56	46	7									10.	45.	55.	0	
337 Devosa	204	51	2	7	59	198	54	7	5.1598	7.9	0.14	2.38	356	−42.415	1.25	1.56	19.	34.	63.	0	X
	195	−62		1		212	−59	1									−23.	−66.	−56.	0	
338 Budrosa	162	20	3	5	63	233	25	5	5.2174	6.0	0.12	2.91	288	−65.671	1.54	1.20	4.2	13.	26.	0	Xk, M
349 Dembowska	153	34	2	6	140	118	27	6	5.1051	8.2	0.09	2.93	33	−67.037	1.31	1.17	5.3	26.	44.	0	R
	330	12		5		298	19	5									1.9	3.1	20.	0	
354 Eleonora	360	18	3	5	155	212	29	6	5.6112	18.4	0.11	2.80	141	−59.549	1.20	1.10	1.9	−0.96	37.	0	Sl
360 Carlova	106	48	3	7	116	346	52	7	3.8775	11.7	0.18	3.00	133	−79.060	1.45	1.26	11.	34.	61.	0	C
372 Palma	65	−3	3	4	189	99	−27	2	2.7936	23.9	0.26	3.14	327	−78.036	1.15	1.18	−0.54	−27.	20.	0	B, BFC
376 Geometria	57	−22	3	2	35	116	−26	2	3.1058	5.4	0.17	2.29	302	−39.549	1.10	1.10	−6.9	−26.	−17.	0	S
	240	−35		2		296	−30	2									−10.	−38.	−30.	0	
382 Dodona	86	66	3	7	58	123	60	7	5.8349	7.4	0.18	3.12	314	−101.073	1.50	1.30	8.9	58.	75.	0	M
416 Vaticana	132	58	2	7	85	78	45	6	4.4673	12.9	0.22	2.79	58	−76.274	1.50	1.20	13.	45.	76.	0	Sl
	310	22		5		250	34	6									5.6	6.9	35.	0	
423 Diotima	155	59	3	7	209	86	48	7	5.0265	11.2	0.04	3.07	70	−73.396	1.15	1.26	6.8	48.	73.	0	C Eos
433 Eros	17	11	4	5	23.6	73	1	4	4.5539	10.8	0.22	1.45	304	−21.099	2.00	1.00	(21)	0.48	18.	5	S Amor
451 Patientia	39	21	3	5	225	315	32	6	2.4638	15.2	0.08	3.06	89	−67.979	1.00	1.00	68.	5.5	36.	0	CU
	163	25		5		75	10	5									68.	9.4	40.	0	
487 Venetia	264	−27	3	2	63	165	−38	2	1.8072	10.2	0.09	2.67	115	−51.436	1.17	1.80	−33.	−42.	−30.	0	S
511 Davida	300	34	4	6	326	181	36	6	4.6789	15.9	0.18	3.17	108	−92.640	1.24	1.12	3.5	18.	51.	0	C
532 Herculina	287	17	3	5	222	174	16	5	2.5519	16.3	0.18	2.77	108	−62.487	1.20	1.20	6.1	−0.084	36.	0	S
534 Nassovia	55	46	3	7	33	324	48	7	2.5346	3.3	0.06	2.88	94	−67.067	1.35	1.45	21.	40.	50.	0	Sq Koronis
	241	49		7		144	47	7									22.	45.	55.	0	

(*continued on next page*)

Table 2 (*continued*)

Asteroid	λ_e	β_e	q	z_e	D	λ_o	β_o	z_o	ν	I	e	A	Ω	$\dot{\Omega}$	a/b	b/c	$\langle\dot{\psi}\rangle$	β_{min}	β_{max}	M	Taxonomy, family
584 Semiramis	113	−47	3	1	54	201	−44	2	4.7347	10.7	0.23	2.37	282	−41.864	1.30	1.20	−15.	−54.	−38.	0	Sl
	335	−50		1		43	−58	1									−17.	−60.	−45.	0	
675 Ludmilla	16	−39	3	2	100	117	−48	1	3.1099	9.8	0.20	2.77	263	−64.613	1.30	1.20	−13.	−49.	−33.	0	S
	210	−52		1		301	−44	2									−15.	−58.	−43.	0	
683 Lanzia	16	−53	3	1	82	135	−68	1	5.0912	18.5	0.05	3.12	260	−64.313	1.40	1.00	−3.9	−71.	−36.	0	C
	190	−53		1		285	−35	2									−3.8	−69.	−34.	0	
694 Ekard	98	40	2	6	91	216	51	7	4.0527	15.8	0.32	2.67	230	−56.843	1.30	1.20	10.	18.	58.	0	CP
	89	−48		1		229	−37	2									−13.	−59.	−33.	0	
704 Interamnia	51	22	3	5	317	127	8	4	2.7500	17.3	0.15	3.07	281	−63.933	1.10	1.10	2.9	4.2	41.	0	B, F
720 Bohlinia	48	41	3	6	34	14	41	6	2.6910	2.4	0.01	2.89	36	−67.212	1.40	1.25	15.	39.	45.	0	Sq Koronis
	236	38		6		198	39	6									14.	35.	41.	0	
776 Berbericia	8	23	3	5	151	292	40	6	3.1299	18.2	0.16	2.93	80	−62.551	1.14	1.24	4.7	1.6	41.	0	Cgh, C
951 Gaspra	19	21	4	5	15.5	125	18	5	3.4081	4.1	0.17	2.21	253	−35.707	1.60	1.10	17.	17.	32.	0	S Flora
1036 Ganymed	208	−76	3	1	38.5	297	−58	1	2.3274	26.6	0.54	2.66	216	−74.660	1.00	1.50	−46.	−86.	−55.	0	S Amor
1223 Neckar	72	45	3	6	22	33	44	6	3.0686	2.6	0.06	2.87	41	−65.698	1.50	1.30	17.	42.	49.	0	S Koronis
	247	42		6		204	43	6									15.	38.	45.	0	
1566 Icarus	214	5	3	4	1.3	127	−13	3	10.5558	22.9	0.82	1.08	88	−24.953	1.23	1.40	−94.	−14.	−4.7	1	SUQ Apollo
1572 Posnania	46	−65	3	1	34	10	−71	1	2.9816	13.3	0.21	3.10	6	−91.781	1.35	1.04	−9.4	−78.	−54.	0	
1580 Betulia	136	22	3	5	3.9	73	−28	2	3.9098	52.1	0.49	2.19	62	−48.739	1.10	1.40	(51)	−29.	77.	4	C Amor
1620 Geographos	55	−46	4	1	2.6	74	−59	1	4.5947	13.3	0.34	1.25	337	−21.974	2.60	1.10	−240.	−59.	−57.	1	S Apollo
1627 Ivar	333	43	3	6	6.9	192	45	6	5.0050	8.4	0.40	1.86	133	−36.703	1.90	1.30	(13)	−0.65	58.	5	S Amor
1685 Toro	210	43	3	6	3	301	51	7	2.3540	9.4	0.44	1.36	274	−28.793	2.10	1.80	430.	51.	52.	2	S Apollo
1862 Apollo	47	−31	3	2	1.4	7	−32	2	7.8275	6.4	0.56	1.47	36	−39.551	2.08	1.80	−87.	−34.	−30.	1	Q Apollo
1980 Tezcatlipoca	334	−66	3	1	6.7	285	−87	1	3.3093	26.9	0.36	1.71	246	−22.242	1.40	1.40	(150)	−87.	−85.	3	Sl, SU Amor
2063 Bacchus	24	−26	3	2	1.2	347	−24	3	1.5337	9.4	0.35	1.08	33	−30.493	2.09	1.06	−460.	−25.	−24.	1	Sq Apollo
2100 Ra-Shalom	73	13	3	5	2.5	261	29	6	1.2121	15.8	0.44	0.83	171	−22.987	1.20	1.30	1300.	29.	30.	2	Xc, C Aten
3103 Eger	10	−50	3	1	2.5	249	−31	2	4.2055	20.9	0.35	1.41	129	−18.656	1.50	1.00	−60.	−40.	−31.	1	Xe, E Apollo
3199 Nefertiti	197	−22	3	3	1.8	223	−1	4	7.9466	33.0	0.28	1.57	340	−17.416	1.10	1.10	−2.8	−39.	12.	0	Sq Amor
3200 Phaeton	97	−11	3	3	5.1	195	−6	4	6.6841	22.2	0.88	1.27	265	−32.454	1.0	1.0	0.0	−33.	11.	0	B, F Apollo
	276	−15		3		4	−18	3									0.0	−37	7	0	
3908 Nyx	43	71	2	7	0.9	136	70	7	5.4224	2.2	0.46	1.93	262	−51.299	1.20	1.00	17.	69.	75.	0	V Amor
	291	69		7		34	68	7									16.	66.	73.	0	
4769 Castalia	235	−56	3	1	1.4	269	−47	1	5.8624	8.9	0.48	1.06	326	−32.846	2.00	1.00	−250.	−49.	−47.	1	Apollo
4957 Brucemurray	358	−50	3	1	3.0	153	−81	1	8.2981	35.0	0.22	1.57	255	−14.031	1.10	1.10	−18.	−84.	−56.	0	S Amor
4979 Otawara	50	−30	3	2	2.0	340	−30	2	8.8671	0.9	0.14	2.17	70	−33.718	1.20	2.30	−13.	−31.	−30.	0	S
5587 1990 SB	253	−60	3	1	6.5	33	−74	1	4.7504	18.1	0.55	2.39	191	−63.957	2.00	1.20	−44.	−77.	−56.	0	Sq Amor
6053 1993 BW3	178	−7	3	4	3.1	219	7	4	9.3257	21.6	0.53	2.15	319	−44.736	1.10	1.50	−1.4	−25.	16.	0	Sq Amor
	354	−16		3		28	−27	2									−6.3	−35.	2.2	0	
6489 Golevka	205	−46	4	1	0.4	352	−46	1	3.9805	2.3	0.61	2.50	211	−155.704	1.20	1.00	−11.	−48.	−44.	0	Q Apollo
25143 Itokawa	39	−87	3	1	0.4	308	−86	1	1.9782	1.7	0.28	1.33	71	−129.424	1.95	1.25	−470.	−87.	−86.	1	S Apollo
	355	−84		1		281	−82	1									−470.	−83.	−82.	1	

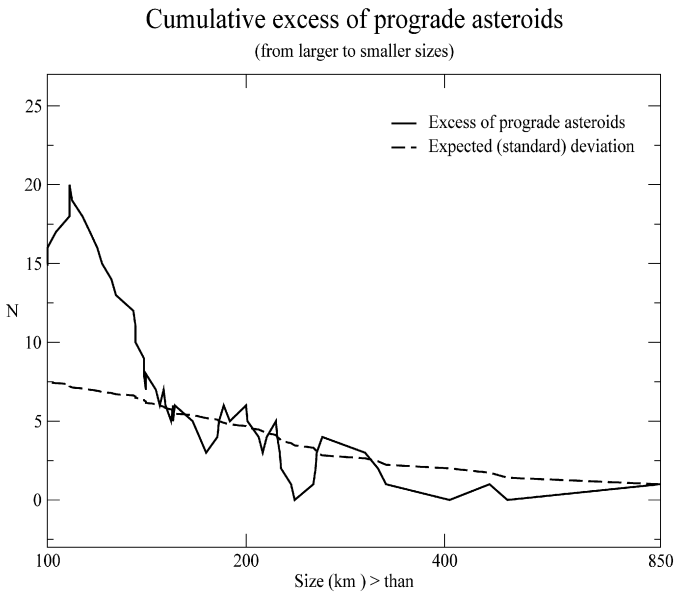

Fig. 2. The figure represents the cumulative excess of prograde asteroids (vs the retrograde one) larger than a given size, as function of the size itself. The standard expected deviation (i.e., the square root of the bodies of known spin vector latitude larger than the corresponding size value) is also represented, for comparison.

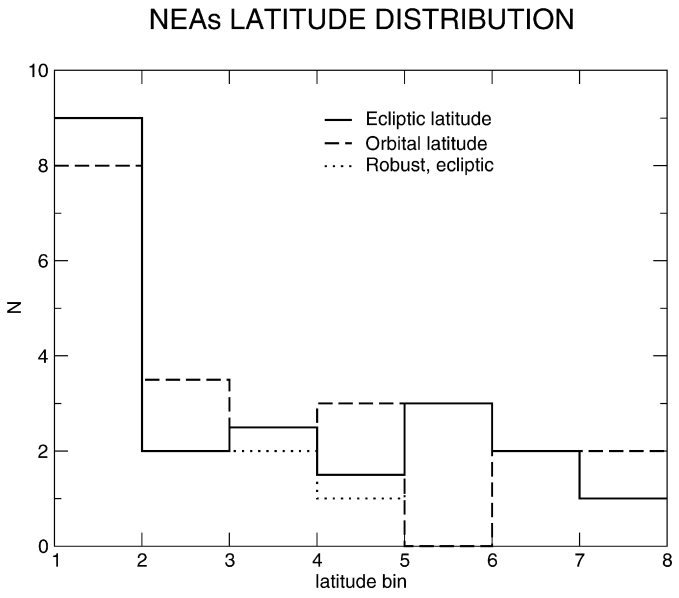

Fig. 3. The histogram shows the latitude distributions for the poles of near-Earth asteroids (NEAs) with the same conventions and symbols as those adopted in Fig. 1.

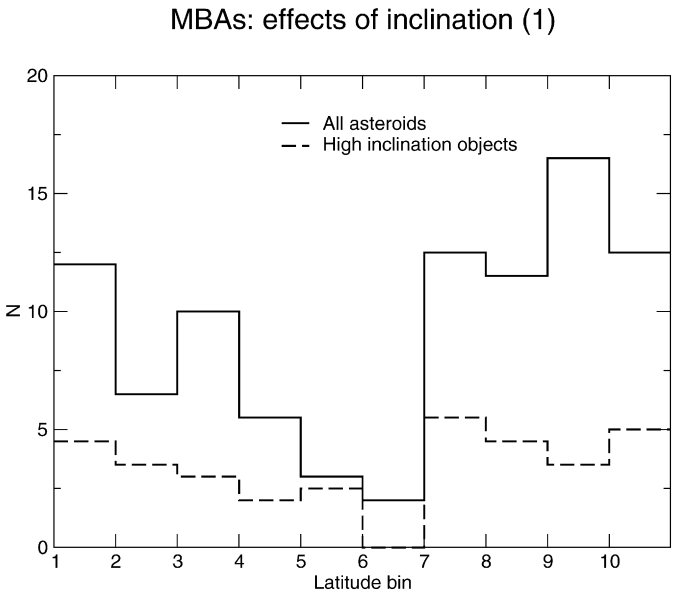

Fig. 4. The histogram compares the latitude distribution for all MBAs with that concerning the high inclination ones ($I > 10°$). The latitude binning is defined in accordance with Skoglov and Erikson (2002), i.e., taking 10 equal spacings in $\sin(\beta)$.

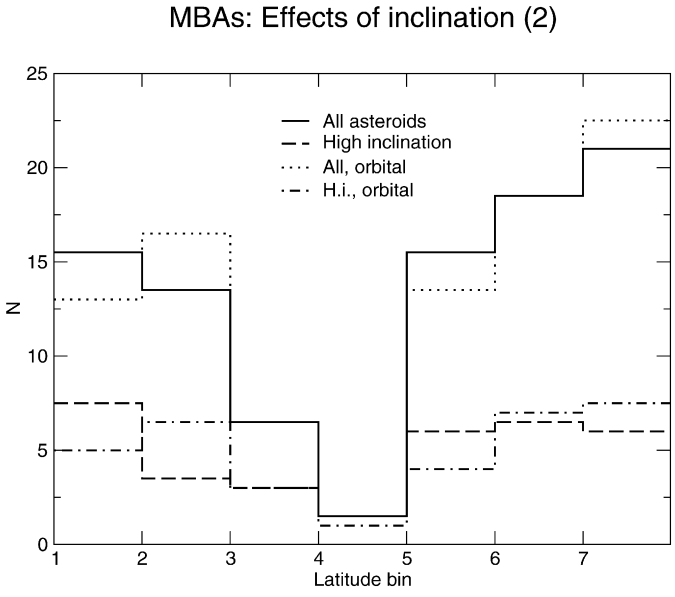

Fig. 5. As in Fig. 4, but the latitude binning is the one usually adopted in the present paper (see caption of Fig. 1). We plot also the corresponding cases where the latitude bin is defined with respect to the asteroid orbital plane.

4.2. The inclination effect

Skoglov and Erikson (2002) claim to have found a correlation between the orbital inclination and the latitude distribution. According to their data the depopulation of close-to-the-ecliptic plane poles is, for the most part, due to the presence of high ($>10°$) inclination bodies. We have redone the same computation using our dataset. We have found no significant correlation between the inclination and the latitude distribution. The only qualitative difference is a better symmetry, in the high-inclination sample, between prograde and retrograde bodies. However, the statistical significance of this difference is low. In Figs. 4 and 5 we compare the latitude distribution for all MBAs with that for the high inclination ones, according both to the latitude binning used in the above quoted paper of Skoglov and Erikson (Fig. 4) and our definition (Fig. 5). Some of the data used in the Skoglov and Erikson analysis has never been published and thus may not be included in our dataset. Without knowing which asteroids were included in their analysis and what pole positions were used, we cannot make a detailed comparison between their results and ours to determine whether the

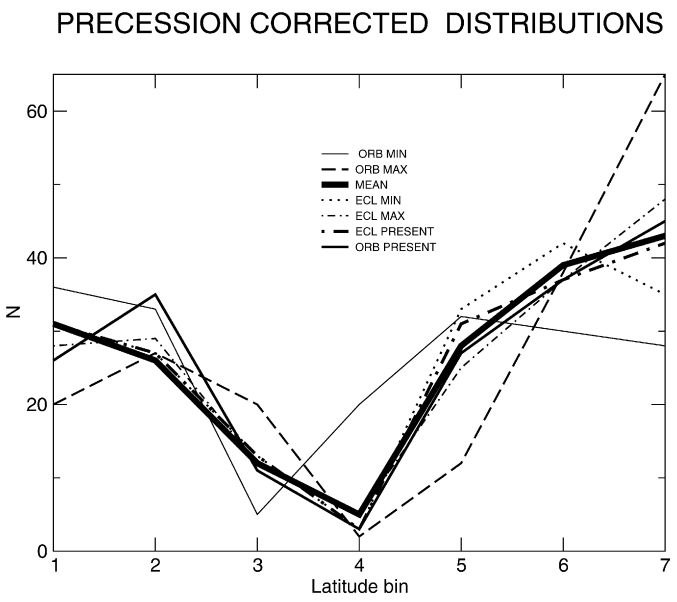

Fig. 6. With the 7-regions latitude binning, we represent the latitude distributions for the cases in which one takes into account the latitude librations. "Ecl" refers always to ecliptic quantities, while "min," "max" and "mean" are referred to the minimum, maximum and mean value of the latitude during its libration period. Note that the ecliptic and orbital latitudes librate around the same central value.

differences in results are due to the data used or to the analysis.

Nevertheless, deeper analysis of this discrepancy and of the related theoretical ideas is required. The underlying ideas are based on the concept of pole precession with time, and on the possible correlations between the properties of this effect (rate and amplitude) and the orbital parameters. For this reason, we have analyzed the precession properties of the objects in our database with a simplified analytical approach (see Appendix B), obtaining the precessional data listed in the general Table 2 (Appendix A).

The analytical model we use, known as the Colombo's top (Colombo, 1966; Peale, 1969; Henrard and Murigande, 1987), is a compromise between the simplistic assumption that the spin axes are fixed in space, and the elaborate numerical integration of the full spin-orbit problem. Thus the results are less accurate, but—in contrast to numerical integration—they can be quickly repeated (or recomputed with new data) by all readers. The Colombo's top model has few limitations: most of all, it excludes a priori all resonances between the orbital motion and precession of the spin axis; it also hinges upon the reliability of proper elements. Nevertheless, the model captures the qualitative features of the spin axis evolution and in typical non-chaotic situations the precession period and amplitude computed according to this model will only be modulated by the oscillations of mean orbital elements around their proper elements values.

This analysis allows us to estimate the amplitude of variation of both ecliptic and orbital spin vector latitudes. In agreement with the conclusions obtained by Skoglov and Erikson as a result of their numerical simulations, we obtain a general correlation between the amplitude of the pole libration with respect to the orbital plane and the inclination. The correlation results from the properties of the roots of Eq. (B.7) in Appendix B. As one can see from the equations presented and from the data (most MBAs have "motion identifier" $M = 0$), this almost linear correlation cannot be extended to the ecliptic latitude in general. Thus, with respect to the orbital latitude, its variation is rather large, and larger for high inclination bodies. The variation of the ecliptic latitude is in general rather small, and not naturally correlated to the inclination. One may plot the latitude distribution taking into account, instead of the present latitude, the minimum, maximum or mean values during the libration. It turns out (Fig. 6) that the distributions of *all* ecliptic latitudes are qualitatively similar, with the same properties; with respect to the distribution of orbital latitudes significant (but obvious) differences are present for the minimum-latitude and maximum-latitude distributions. Due to the relevant variation amplitudes the features, in particular the central depleted region—are moved to the previous or to the following latitude bin. All these results show that the present ecliptic latitude distribution is fully representative of the distribution observed at different times. Due to statistical considerations (the phases are randomly distributed) also the present orbital latitude distribution is very similar to that related to the ecliptic. Both distributions are very similar to that obtained computing the mean ecliptic or orbital latitudes (the mean values are the same). Finally, within our model, we have looked for the correlation between the initial (i.e., present) latitude and its variation amplitude. According to Skoglov and Erikson (2002) small (in absolute value) orbital latitudes entail larger variations. They claim also that a similar, even if weaker, correlation exists with respect to the ecliptic latitude value (more exactly, their analysis concerns trigonometric functions of the quantities above). This effect might be responsible of the scarcity of bodies with latitudes close to zero.

In Figs. 7 and 8 we plot our results, for the orbital and ecliptic latitudes. In this latter case, to have a more direct insight into the possible inferences related to the observed latitude distribution, we plot $\cos(\beta)\Delta\beta \simeq \Delta \sin(\beta)$ versus $\sin(\beta)$. In fact the binning we use is in terms of $\sin(\beta)$, which is the relevant quantity whenever we wish to estimate the deviations from isotropy ($\cos(\beta)\,\mathrm{d}\beta\,\mathrm{d}\lambda$ is the surface element on a unit sphere, where λ and β are the coordinates). With respect to the orbital latitudes, a weak correlation can be found, while no one comes out in the case of ecliptic latitudes. The effect seems unable to explain the depletion of close-to-zero latitudes.[1]

Since the libration amplitudes in the ecliptic frame are generally smaller than in the orbital frame we may conclude that the precession takes place around the normal to the ecliptic rather than around the normal to the orbit.

[1] At this place we take also an opportunity to indicate a weak point in the argument provided by Skoglov and Erikson (2002). Using an analogue of Eq. (B.5) they claimed that $\dot{X}$ is small for large $|X|$, hence most of the time is spent by spin axes close to the maximum of $|X|$. But the principal reason of the small $\dot{X}$ value close to both exteemes is $\sin\phi \approx 0$, and any asymmetry between $\dot{X}$ at $X_{\max}$ and $X_{\min}$ is also flattened by the fact that $\dot{\phi}$ is proportional to X as seen in Eq. (B.4).

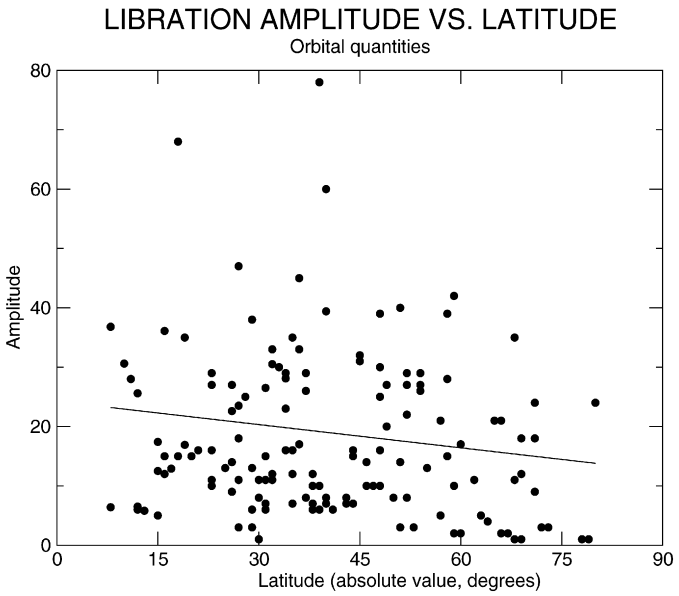

Fig. 7. The plot represents the libration amplitude vs the present orbital latitude (absolute value, degrees). A rough r.m.s. linear fit is represented, for comparison.

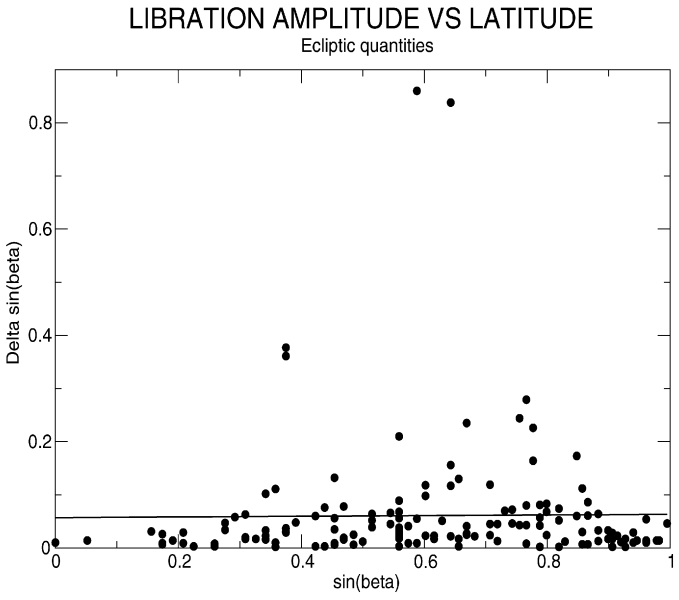

Fig. 8. The plot is similar to Fig. 7, but is referred to ecliptic quantities. Moreover the amplitude is expressed in terms of $\cos(\beta)\Delta\beta \simeq \Delta\sin(\beta)$ and, in the abscissa, $\sin(\beta)$ is represented.

4.3. Longitude distributions

We have examined the distribution of longitudes for both MBAs and NEAs. The distribution of longitudes for MBAs (see Fig. 9) is not far from being uniform, with only very moderate gaps in the regions 120/180° and 300/360°. These dips are only of about "1-σ" significance, only just the level of deviations expected from a random distribution. The relevance of the irregularities in the longitude distribution claimed by Samarasinha and Karr (1998) is thus not confirmed. In turn, NEAs appear to exhibit two sharp maxima (Fig. 9), in the regions 0/60° and 180/240°. Again, they are only of about "1-σ"

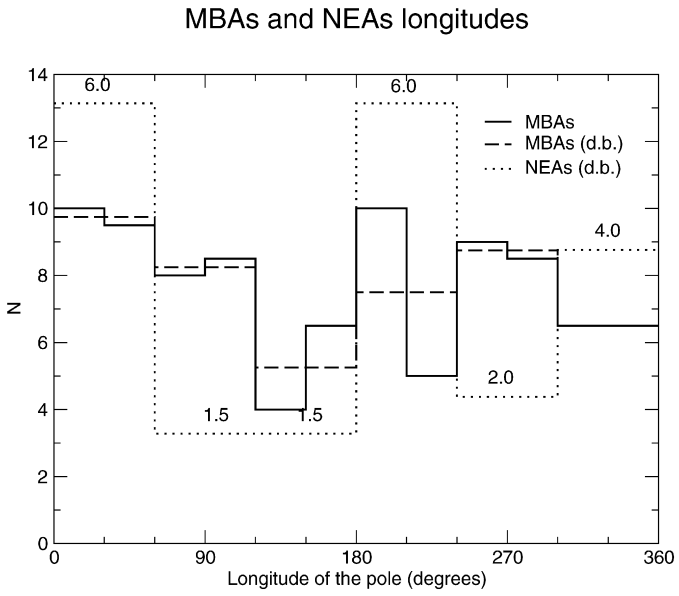

Fig. 9. The histogram shows the distribution of the longitude for the poles of 92 MB and 21 near-Earth asteroids. The MBAs (solid line) are divided into twelve equally spaced bins (again, with the same convention with respect to double values). We plot also the distribution divided into six double-sized bin (60° each, long-dashed line). For sake of comparison, the values are divided per two. The NEA distribution (dotted line) is represented with double-sized bins and normalized to the same value as MBAs. The true numbers are also explicitly written.

significance and thus more likely just random fluctuations in the distribution.

The results presented above may be also relevant in connection with other recent results and theoretical analyses. In particular, YORP effect has been claimed to have relevant observable consequences (Rubincam, 2000; Slivan, 2002; Vokrouhlicky et al., 2003). In principle, these processes can lead to clustering of the spin vector directions; they might also contribute to the depopulation of poles close to the ecliptic plane. Note, however, that most MBAs in our sample are too large to be substantially affected by solar radiation, although some minor *statistical* effect might still be apparent. This point will be discussed also in Section 4.4.

4.4. Bi-dimensional distributions

In Fig. 10 we give a bi-dimensional representation of asteroid poles.

In the figure we present, with separate symbols, the Koronis family asteroids and all the non-Koronis MBAs smaller than 100 or 60 km. These rather larger limits for "small" bodies have been chosen in order to have a significant number of bodies in the sample. The figure confirms the previously discussed scenario and the peculiar properties, already known, of the so-called Slivan asteroids (the stars in the top half and at the bottom). However one can note that the few "small" bodies for which $D < 60$ km seem overdense in the extreme latitude bins, and underdense (also in comparison to the whole sample) in the latitude region close to 0°, consistently with previous theories (Vokrouhlicky et al., 2003).

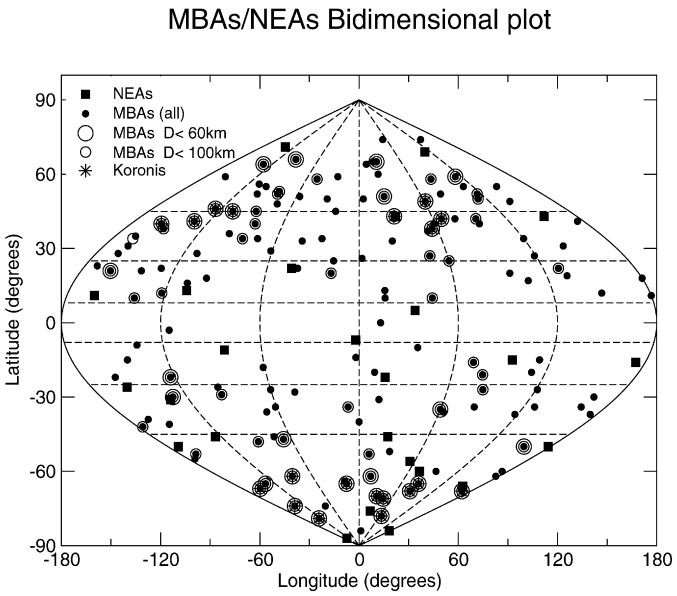

Fig. 10. The figure represents, in a sinusoidal equal-area cartographic representation, the bi-dimensional pole distributions of asteroids. The vertical dashed lines separate the latitude-bins previously discussed, and the horizontal curves separate the longitude-bins (here the longitude values range from −180° to 180°, thus the values of Fig. 1 have to be diminished by 180°). The NEAs are represented as filled squares, while the MB asteroids are represented as small circles. Koronis family asteroids are starred. The MB-non-Koronis asteroids with a estimated diameter smaller than 100 km are encircled. Those whose diameter is also smaller than 60 km are encircled twice. The asteroids with ambiguous pole determination (see text) are represented twice.

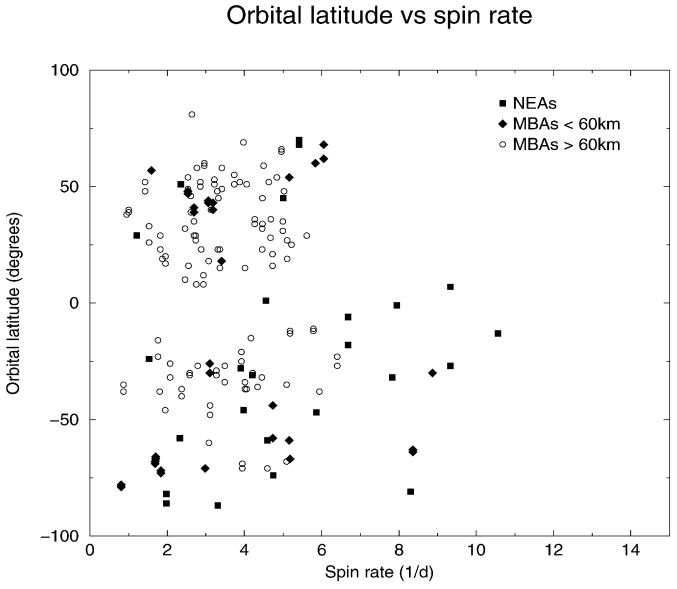

Fig. 11. We plot the latitude—computed with respect to the orbital plane—vs the spin rate of the asteroids in our sample. NEAs and MBAs smaller than 60 km are plotted with separate symbols (filled squares and diamonds, respectively). The distribution of "small" bodies (NEAs and small MBAs) seems marginally different from that of the large bodies.

Finally, we have performed a different test, plotting the latitude vs the spin rate. The rationale of this comparison follows from a general overview of the YORP effect (see, for instance, Capek and Vokrouhlicky, 2004, and references therein). Even if the present understanding of the effect entails different possible evolutions of the spin vector, also in connection with competing dynamical effects (Vokrouhlicky et al., 2006), and depending on the shape of the body, some general features come out: the effects on the spin rates and on the pole orientation act together, on similar timescales. Depending also on the initial conditions, the spin rate may significantly decrease or increase, while the pole orientations are often clustered close to both poles of the orbital plane. Thus, the bodies which have been intensely affected by YORP should exhibit a structure in the spin–latitude plane, the clustering towards the poles being related to a significant increase or decrease of the period. In Fig. 11 we plot the latitude computed with respect to the orbital plane (i.e., the obliquity) vs the spin rate. We represent with different symbols the NEAs, the MBAs smaller than 60 km ("small MBAs") and the "large MBAs" (larger than 60 km). The figure shows some differences between the behavior of NEAs + "small MBAs" and "large" bodies; among the small ones we find some fast spinners (mainly NEAs) which are more abundant at small obliquities, while the high—positive or negative—obliquities are typical of slower spins. We do not find the combination very-fast spin and high obliquity. However, one may suggest that small bodies have, as their original properties, a fast spin and that a further increase due to YORP may rapidly cause their bursting fission. Thus the structure of "small" bodies might be consistent with the consequences of YORP effect. Note also that most of the fast spinners are retrograde. Since most of the involved bodies are NEAs, the finding, even if, in principle interesting, may be not independent on the already known excess of retrograde NEAs (La Spina et al., 2004b).

No structure is present for large bodies. However, the differences among the samples are not sufficient to show an unambiguous fingerprint of the YORP effect in the general spin vector properties. Note also that, apart from NEAs, the size of the "small" asteroids in our sample is often larger (usually 50–60 km) than the 40 km, upper limit sometimes assumed in the literature for a significant YORP-driven evolution (see the references above). Moreover we have to remark that the presence of some NEAs with short period and small latitude might be also due to the dynamical disturbances of a recent close encounter with some of the inner planets. The present results can be considered as a further suggestion of the potential relevance of spin vector data, especially if extended to include smaller MBAs and members of asteroid dynamical families, other than Koronis.

5. Conclusions

A qualitative analysis of the latitude data shows an essential difference between MBAs and NEAs with respect to prograde vs retrograde rotations. A dynamical "filtering" of MBAs transferred by resonance into Earth-crossing orbits appears to explain this difference (La Spina et al., 2004b), due to the Yarkovsky effect (Vokrouhlicky, 1998, 1999; Vokrouhlicky and Farinella, 1998; Spitale and Greenberg, 2001; Morbidelli and Vokrouhlicky, 2003). Among MBAs, there is no significant prograde excess among the very largest asteroids, instead there is only a moderately significant excess in the limited size range

from 100 to 150 km diameter. This latter excess is without physical explanation.

We confirm the ecliptic-plane depopulation, already found by past analyses. A final explanation is, in our opinion, not available. Selection effects, the role of inclination, and YORP effects might be invoked; however, according to the previous discussion, their relevance can be questioned.

We do not confirm a statistically significant clustering in longitude of poles of either MBAs or NEAs.

The analysis of the bi-dimensional distribution might be useful for understanding the role of various known and new effects. Note that a complex structure for the pole angular distribution might even affect the spin distribution (La Spina et al., 2002, 2004a).

There are probably several different mechanisms shaping the distribution of spin rates of small MBAs and NEAs, leading us to expect that the distributions may be non-Maxwellian, and possibly even bi-modal. For a discussion see Pravec et al. (2002, and references therein). Also, due to the YORP effect we may expect a correlation between spin rates and pole orientations.

However, note that these effects are presumably dominant for small bodies, while the present dataset contains, at least for MBAs, mainly large or medium-sized bodies. We remark that further spin vector data are urgently needed, especially for NEAs and small and family MBAs.

Acknowledgments

A.L.S. and P.P. have been supported by INAF and MIUR grants, A.K. by the Polish Grant 1 P03D 008 26. The research by P. Pravec has been supported by the Grant Agency of the Academy of Sciences of the Czech Republic, Grant A3003204. The research by A.W. Harris was supported by the NASA Planetary Geology and Geophysics Program, NAG5-13244.

Appendix A

Table 2 contains summary of the data used in our analysis for 113 asteroids. The information included is:

Asteroid — the permanent number and name (or provisional designation)

λ_e, β_e — ecliptic longitude and latitude of the asteroid pole (in degrees)

q — reliability code for pole determination: 4—excellent determination, 3—very good determination, 2—good determination with two equally probable solutions

z_e — zone referred to the ecliptic latitude of the pole

D — diameter (km)

λ_o, β_o — orbital longitude and latitude of the asteroid pole (degrees)

z_o — zone referred to the orbital latitude of the pole

ν — asteroid rotational frequency in cycles per day, i.e., the inverse of the rotation period

I — inclination of the asteroid orbit (degrees)

e — eccentricity of the asteroid orbit

A — semimajor axis of the asteroid orbit (AU)

Ω — proper orbital node (degrees)

$\dot{\Omega}$ — proper rate of the orbital node ($''$/y)

a/c, b/c — asteroid semiaxes ratio

$\langle\dot{\psi}\rangle$ — mean angular rate of the precession argument in $''$/y; the values in brackets stand for the frequency of libration in λ_o when $\langle\dot{\psi}\rangle = -\dot{\Omega}$. The details are given in Appendix B

β_{min}, β_{max} — minimum and maximum values of the spin axis latitude (in degrees) with respect to the orbital plane; see Appendix B

M — spin axis motion type (see Appendix B)

taxonomy, family — this column contains additional information about taxonomic type of the asteroid and indicates the membership in the dynamical family.

Appendix B

The Colombo's top is a basic model for the precession of the spin axis if we assume that: (i) the angular momentum vector permanently coincides with the maximum inertia axis, (ii) the asteroid moves on a heliocentric elliptic orbit with eccentricity e and constant inclination I, and the orbit's line of nodes rotates with a constant rate $\dot{\Omega}$ in some invariant plane, (iii) the torque due to the Sun can be averaged over the orbital and revolution periods (Colombo, 1966; Peale, 1969; Henrard and Murigande, 1987). Introducing a canonically conjugate pair (φ, X), where the angle

$$\varphi = 90^\circ - \lambda_o = \psi + \Omega, \tag{B.1}$$

is the sum of the usual precession angle ψ (cf. Kinoshita, 1977; Laskar and Robutel, 1993) and the longitude of the orbital ascending node Ω, and the momentum is the cosine of the spin axis colatitude in the orbital frame

$$X = \cos(90^\circ - \beta_o) = \sin\beta_o,$$

we can write the Hamiltonian function of the Colombo's top

$$\begin{aligned}\mathcal{H} &= \frac{\alpha}{2}X^2 + \cos I\,\dot{\Omega}X + \sin I\,\dot{\Omega}\sqrt{1-X^2}\cos\varphi \\ &= E = \text{const.}\end{aligned} \tag{B.2}$$

The parameter α is a function of orbital elements and of the body shape; assuming the homogeneous ellipsoid model for the moments of inertia, we obtain

$$\alpha = \frac{3}{2}\frac{k^2 M_\odot}{2\pi\nu A^3(1-e^2)^{3/2}}\left(\frac{1}{2} - \frac{1}{[1+(a/b)^2](b/c)^2}\right), \tag{B.3}$$

where $a \geqslant b \geqslant c$ are the semiaxes of the ellipsoid, $M_\odot$ is the solar mass, k stands for the Gaussian constant, A is the proper semimajor axis of the orbit, and ν is the asteroid rotation frequency (in cycles per time unit). Thus all quantities present in $\mathcal{H}$ can be computed from the data given in Table 2. The initial conditions φ_0 and X_0 can also be computed from λ_o and β_o taken from Table 2; they serve to evaluate the value of E.

Canonical equations of motion derived from the Hamiltonian (B.2) take the form

$$\frac{d\varphi}{dt} = \left(\alpha - \frac{\dot{\Omega}\sin I}{\sqrt{1-X^2}}\cos\varphi\right)X + \dot{\Omega}\cos I, \tag{B.4}$$

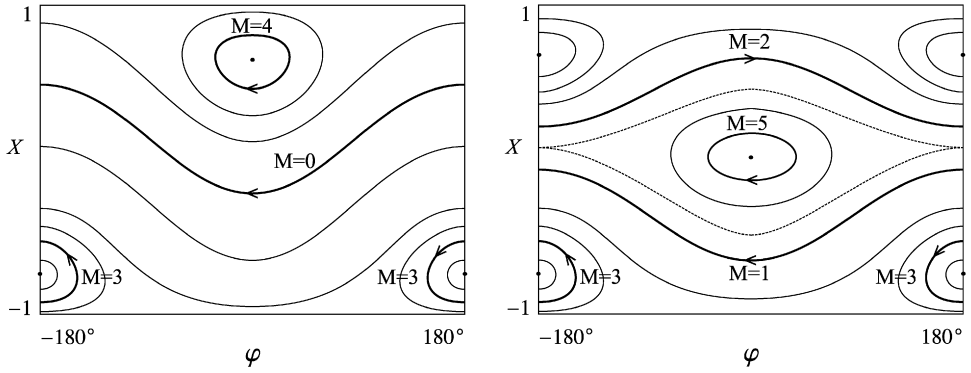

Fig. 12. Generic types of spin axis motion in the Colombo's top problem. Bold lines are exemplary curves labeled by the values of M. The dashed line refers to the separatrix of the resonance between the spin axis and the orbital node.

$$\frac{\mathrm{d}X}{\mathrm{d}t} = \dot{\Omega}\sin I\sqrt{1-X^2}\sin\varphi. \tag{B.5}$$

Solving Eq. (B.2) for $\cos\varphi$ and using the solution to remove the dependence of $\dot{X}$ on φ, we obtain Eq. (B.5) reduced to a quadrature

$$t_2 - t_1 = \frac{2}{\alpha}\int_{X(t_1)}^{X(t_2)} \frac{\mathrm{d}X}{\sqrt{W(X,E)}}, \tag{B.6}$$

where

$$W(X,E) = -X^4 - 4\frac{\dot{\Omega}\cos I}{\alpha}X^3 + 4\frac{E-\dot{\Omega}^2}{\alpha}X^2 + 8\frac{E\dot{\Omega}\cos I}{\alpha^2}X + 4\frac{(\sin I)^2\dot{\Omega}^2 - E^2}{\alpha^2}. \tag{B.7}$$

W is a fourth degree polynomial in X and it may have up to four real roots

$$X_1 \leqslant X_2 \leqslant X_3 \leqslant X_4,$$

that are the values of X, for which $\dot{X} = 0$. In other words, if $X_i \leqslant X_0 \leqslant X_{i+1}$, then X_i and X_{i+1} are the extremes of $X(t)$ for the given X_0 and E. The orbital latitude oscillates within the bounds set by X_i and X_{i+1}. Table 2 provides the minimum and maximum latitudes with respect to the orbital plane

$$\beta_{\min} = \arcsin X_i, \qquad \beta_{\max} = \arcsin X_{i+1}, \tag{B.8}$$

that the spin axis may attain within the Colombo's top approximation.

Fig. 12 presents generic types of the spin axis motion plotted as the curves of constant $\mathcal{H}$ on the phase plane (φ, X). Six types of the $X(\varphi)$ curves are labeled by the motion type identifier M. For each set of rotational data given in Table 2, the relevant value of M is given to facilitate the interpretation of other results. Knowing the type of motion, one may quickly compute the extreme values of β_e: observing that the extremes of the spin axis latitude with respect to the orbit are attained either at $\varphi = 0°$ (i.e., $\lambda_o = 90°$ and $\psi = -\Omega$), or at $\varphi = \pm 180°$ (where $\lambda_o = 270°$), one can easily deduce the following rules to compute the extremes of latitude referred to the ecliptic $B_{\max} = \max(\beta_e)$ and $B_{\min} = \min(\beta_e)$: let

$$B_1 = \begin{cases} \arcsin\big[\sin(\beta_{\min} + I)\big] & \text{for M} = 0, 1, 4, 5, \\ \arcsin\big[\sin(\beta_{\min} - I)\big] & \text{for M} = 2, 3, \end{cases} \tag{B.9}$$

and

$$B_2 = \begin{cases} \arcsin\big[\sin(\beta_{\max} + I)\big] & \text{for M} = 2, 4, 5, \\ \arcsin\big[\sin(\beta_{\max} - I)\big] & \text{for M} = 0, 1, 3. \end{cases} \tag{B.10}$$

Then

$$B_{\max} = \max(B_1, B_2), \qquad B_{\min} = \min(B_1, B_2). \tag{B.11}$$

It is worth noting that the point of maximum latitude in the orbital frame can be either the maximum or the minimum latitude in the ecliptic plane and vice versa. This is related to the fact that the sum or difference of $\beta \pm I$ can be larger than 90° in the absolute value.

The period of oscillations in X, i.e., the period of latitude variations, can be evaluated from

$$T_X = \frac{4}{\alpha}\int_{X_i}^{X_{i+1}} \frac{\mathrm{d}X}{\sqrt{W(X,E)}}. \tag{B.12}$$

This integral can be either expressed in terms of the complete elliptic integral of the first kind or evaluated by numerical quadratures. The former approach, that was actually applied to compute the values given in Table 2, requires a careful identification of the ordering of the roots with respect to X_0 (Byrd and Friedman, 1954), so we checked each result with a numerical integration of Eqs. (B.4) and (B.5). The period T_X is equal to the period of the angle φ, hence it is also the period of λ_o.

It is important to distinguish the circulation case M = 0, 1, 2, when $0° \leqslant \varphi < 360°$, from the libration of φ (M > 2), when the angle oscillates around 0° or 180° (Henrard and Murigande, 1987). For the circulation case mean rate of the precession angle $\langle\dot{\psi}\rangle$ is, according to the definition (B.1),

$$\langle\dot{\psi}\rangle = \operatorname{sgn}\big[\dot{\varphi}(\varphi_0, X_0)\big]\frac{2\pi}{T_X} - \dot{\Omega}. \tag{B.13}$$

The precession rate in Table 2 is computed according this formula (after changing units to arcseconds per year). The sign of $\dot{\varphi}$ is evaluated from the right-hand side of Eq. (B.4) using φ_0 and X_0; it does not change during the motion if φ circulates. In the libration case, λ_o has no secular drift with respect to the ascending node, hence

$$\langle\dot{\psi}\rangle = -\dot{\Omega}, \tag{B.14}$$

and in this case, instead of duplicating the value from another column, we exceptionally replace $\langle\dot{\psi}\rangle$ in Table 2 with the values of the libration frequency

$$\nu = \frac{2\pi}{T_X}, \tag{B.15}$$

always taken positive, regardless of the actual libration sense on the (φ, X) plane, and enclosed in brackets "( )" to avoid confusion.

References

Barucci, M.A., Bockelee-Morvan, D., Brahic, A., Clairemidi, S., Lecacheux, J., Roques, F., 1986. Asteroid spin axes: Two additional pole determination and theoretical implications. Astron. Astrophys. 163, 261–268.

Bertotti, B., Farinella, P., Vokrouhlicky, D., 2003. Physics of the Solar System. Kluwer Academic, Dordrecht.

Bottke, W.F., Morbidelli, A., Jedicke, R., Petit, J.-M., Levison, H., Metcalfe, T.S., 2002. Debiased orbital and absolute magnitude distribution of near-Earth objects. Icarus 156, 399–433.

Byrd, P.F., Friedman, M.D., 1954. Handbook of Elliptic Functions for Engineers and Physicists. Springer-Verlag, Berlin.

Capek, D., Vokrouhlicky, D., 2004. The YORP effect with finite thermal conductivity. Icarus 172, 526–536.

Colombo, G., 1966. Cassini's second and third laws. Astron. J. 71, 891–896.

Davis, D.R., Weidenschilling, S.J., Farinella, P., Paolicchi, P., Binzel, R.P., 1989. Asteroid collisional history: Effects on sizes and spins. In: Binzel, R.P., Gehrels, T., Shapley Matthews, M. (Eds.), Asteroids II. Arizona Univ. Press, Tucson, pp. 805–826.

Davis, D.R., Durda, D.D., Marzari, F., Campo Bagatin, A., Gil-Hutton, R., 2002. Collisional evolution of small-body populations. In: Bottke, W.F., Paolicchi, P., Binzel, R.P., Cellino, A. (Eds.), Asteroids III. Arizona Univ. Press, Tucson, pp. 545–558.

Drummond, J.D., Weidenschilling, S.J., Chapman, C.R., Davis, D.R., 1988. Photometric geodesy of main-belt asteroids. II. Analysis of lightcurves for poles, periods and shapes. Icarus 76, 19–77.

Drummond, J.D., Weidenschilling, S.J., Chapman, C.R., Davis, D.R., 1991. Photometric geodesy of main-belt asteroids. IV. An updated analysis of lightcurves for poles, periods and shapes. Icarus 89, 44–64.

Henrard, J., Murigande, C., 1987. Colombo's top. Celest. Mech. 40, 345–366.

Kinoshita, H., 1977. Theory of the rotation of the rigid Earth. Celest. Mech. 15, 277–326.

Laskar, J., Robutel, P., 1993. The chaotic obliquity of the planets. Nature 361, 608–612.

La Spina, A., Paolicchi, P., Kryszczyńska, A., Pravec, P., 2002. Pole anisotropy and spin statistics. In: ACM 2002, Proceedings. ESA SP-500, pp. 529–532.

La Spina, A., Paolicchi P., Kryszczyńska, A., Pravec, P., 2004a. Distribution of spin vectors: Differences between main belt and near-Earth asteroids longitudes. In: Planetary Science: Fifth Italian Meeting (Gallipoli 2003), Proceedings, pp. 151–154.

La Spina, A., Paolicchi, P., Kryszczyńska, A., Pravec, P., 2004b. Retrograde spins of near-Earth asteroids from the Yarkovsky effect. Nature 428, 400–401.

Magnusson, P., 1986. Distribution of spin axes and senses of rotation for 20 large asteroids. Icarus 68, 1–39.

Magnusson, P., 1989. Pole determinations of asteroids. In: Binzel, R.P., Gehrels, T., Shapley Matthews, M. (Eds.), Asteroids II. Arizona Univ. Press, Tucson, pp. 1180–1186.

Magnusson, P., 1990. Spin vectors of 22 large asteroids. Icarus 85, 229–240.

Marchi, S., Morbidelli, A., Paolicchi, P., Lazzarin, M., Magrin, S., 2005. Origin of NEAs: Hints based on taxonomy and dynamics of peculiar objects. In: ACM 2005, Búzios, Brazil.

Michałowski, T., Kwiatkowski, T., Kaasalainen, M., Pych, W., Kryszczyńska, A., Dybczyński, P.A., Velichko, F.P., Erikson, A., Denchev, P., Fauvaud, S., Szabo, Gy.M., 2004. Photometry and models of selected main belt asteroids. I. 52 Europa, 115 Thyra, and 382 Dodona. Astron. Astrophys. 416, 353–366.

Morbidelli, A., Vokrouhlicky, D., 2003. The Yarkovsky-driven origin of near-Earth asteroids. Icarus 163, 120–134.

Paolicchi, P., Burns, A., Weidenschilling, S.J., 2002. Side effects of collisions: Spin rate changes, tumbling rotation states, and binary asteroids. In: Bottke, W.F., Paolicchi, P., Binzel, R.P., Cellino, A. (Eds.), Asteroids III. Arizona Univ. Press, Tucson, pp. 501–516.

Peale, S.J., 1969. Generalized Cassini's laws. Astron. J. 74, 483–489.

Pravec, P., Harris, A.W., Michalowski, T., 2002. Asteroid rotations. In: Bottke, W.F., Paolicchi, P., Binzel, R.P., Cellino, A. (Eds.), Asteroids III. Arizona Univ. Press, Tucson, pp. 113–122.

Rubincam, D.P., 2000. Radiative spin-up and spin-down of small asteroids. Icarus 148, 2–11.

Samarasinha, N.H., Karr, T., 1998. Orientation of asteroidal spin vectors. Bull. Am. Astron. Soc. 30, 1035.

Skoglov, E., Erikson, A., 2002. Influence of the orbital evolution of main belt asteroids on their spin vectors. Icarus 160, 24–31.

Slivan, S.M., 2002. Spin vector alignment of Koronis family asteroids. Nature 419, 49–51.

Spitale, J., Greenberg, R., 2001. Numerical evaluation of the general Yarkovsky effect: Effects on semimajor axis. Icarus 149, 222–234.

Vokrouhlicky, D., 1998. Diurnal Yarkovsky effect as a source of mobility of meter-sized asteroidal fragments. I. Linear theory. Astron. Astrophys. 335, 1093–1100.

Vokrouhlicky, D., 1999. A complete linear model for the Yarkovsky thermal force on spherical asteroid fragments. Astron. Astrophys. 344, 362–366.

Vokrouhlicky, D., Farinella, P., 1998. The Yarkovsky seasonal effect on asteroidal fragments: A non-linearized theory for the plane–parallel case. Astron. J. 116, 2032–2041.

Vokrouhlicky, D., Nesvorny, D., Bottke, W.F., 2003. The vector alignments of asteroid spins by thermal torques. Nature 425, 147–151.

Vokrouhlicky, D., Nesvorny, D., Bottke, W.F., 2006. Secular spin dynamics of inner main-belt asteroids. Icarus 184, 1–28.

Zappala, V., Knezevic, Z., 1984. Rotation axes of asteroids: Results for 14 objects. Icarus 59, 435–455.